The Termination of the 1997–98 El Niño. Part II: Mechanisms of Atmospheric Change

GABRIEL A. VECCHI

NOAA/Geophysical Fluid Dynamics Laboratory, Princeton, New Jersey, and UCAR Visiting Scientist Program, Boulder, Colorado

(Manuscript received 11 February 2005, in final form 19 December 2005)

ABSTRACT

The mechanisms that drove zonal wind stress (τ^x) changes in the near-equatorial Pacific at the end of the extreme 1997–98 El Niño event are explored using a global atmospheric general circulation model. The analysis focuses on three features of the τ^x evolution between October 1997 and May 1998 that were fundamental in driving the oceanic changes at the end of this El Niño event: (i) the southward shift of near-date-line surface zonal wind stress (τ^x) anomalies beginning November 1997, (ii) the disappearance of the easterly τ^x from the eastern equatorial Pacific (EEqP) in February 1998, and (iii) the reappearance of easterly τ^x in the EEqP in May 1998. It is shown that these wind changes represent the deterministic response of the atmosphere to the observed sea surface temperature (SST) field, resulting from changes in the meridional structure of atmospheric convective anomalies in response to the seasonally phase-locked meridional movement of the warmest SST.

The southward shift of the near-date-line τ^x anomalies at the end of this El Niño event was controlled by the seasonal movement of the warmest SST south of the equator, which—both directly and through its influence on the atmospheric response to changes in SST anomaly—brought the convective anomalies from being centered about the equator to being centered south of the equator. The disappearance (reappearance) of easterly EEqP τ^x has only been evident in extreme El Niño events and has been associated with the development (northward retreat) of an equatorial intertropical convergence zone (ITCZ). The disappearance/return of EEqP easterly τ^x arises in the AGCM as the deterministic response to changes in the SST field, tied principally to the changes in climatological SST (given time-invariant extreme El Niño SSTA) and not to changes in the underlying SSTA field. The disappearance (return) of EEqP easterly τ^x in late boreal winter (late boreal spring) is a characteristic atmospheric response to idealized extreme El Niño SST anomalies; this suggests that the distinctive termination of the 1997–98 El Niño event is that to be expected for extreme El Niño events.

1. Introduction

Understanding the mechanisms that control the phase changes of the El Niño–Southern Oscillation (ENSO) phenomenon is of both scientific interest and forecast significance. The coupled ocean–atmosphere interactions resulting in El Niño equatorial Pacific sea surface temperature anomaly (SSTA) changes remain an area of active research [see the special issue of *Journal of Geophysical Research*, 1998, Vol. 103, No. C7, and Wang and Picaut (2004) for reviews of recent El Niño research]. The El Niño of 1997–98 was one of the strongest events on record, and its evolution was well observed and has received significant scientific attention (e.g., McPhaden 1999; Takayabu et al. 1999; Wang and Weisberg 2000; Picaut et al. 2002; Boulanger et al. 2004; Lengaigne et al. 2004; Vecchi and Harrison 2006, henceforth VH06; Zhang and McPhaden 2006; Vecchi et al. 2006), and was problematic for many El Niño forecast systems (see Barnston et al. 1999; Landsea and Knaff 2000).

The termination of the 1997–98 El Niño was both distinctive and dramatic. In late 1997 the eastern equatorial Pacific (EEqP) thermocline began to shoal, as has been observed prior to the termination of all El Niño events (e.g., Harrison and Vecchi 2001; Zelle et al. 2004; Zhang and McPhaden 2006). As the EEqP thermocline shoaling continued through April 1998, a very unusual situation developed: the normal easterlies in the EEqP disappeared and decoupled the cooling subsurface from the warm surface ocean (VH06). This led to an atypical period of extremely warm EEqP SST overlying anomalously cool subsurface waters (e.g.,

Corresponding author address: Dr. Gabriel A. Vecchi, NOAA/Geophysical Fluid Dynamics Laboratory, Princeton University, Forrestal Campus, Rte. 1, P.O. Box 308, Princeton, NJ 08542-0308.
E-mail: Gabriel.A.Vecchi@noaa.gov

McPhaden 1999; Harrison and Vecchi 2001). This extraordinary set of conditions persisted until May 1998, at which point the equatorial easterly wind returned and there was a dramatic cooling of EEqP SST—a cooling that exceeded 4°C over two weeks (see McPhaden 1999).

Through the analysis of a series of ocean general circulation model (OGCM) experiments, VH06 identify three particular changes in the tropical Pacific surface zonal wind stress (τ^x) field that were instrumental in controlling the peculiar termination of the 1997–98 El Niño: (i) a southward shift of the near-date-line westerly τ^x anomalies (τ^xa) beginning November 1997, which drove the EEqP thermocline shoaling; (ii) the disappearance of the climatological EEqP easterlies in February 1998, which decoupled the EEqP surface from the cooling subsurface; and (iii) the sudden return of the EEqP easterlies in May 1998, which led to the sensational termination of the event. This manuscript focuses on the changes in SST that resulted in these τ^x features, using a series of global atmospheric general circulation model (AGCM) experiments.

The southward shift of equatorial near-date-line τ^xa is a robust feature in boreal winter of El Niño years (e.g., Harrison 1987; Harrison and Larkin 1998; Harrison and Vecchi 1999; Larkin and Harrison 2002), and the resulting reduction of equatorial τ^xa can drive strong thermocline shoaling in the EEqP (e.g., Harrison and Vecchi 1999; Vecchi and Harrison 2003; VH06). The meridional shift in the location of interannual westerly anomalies occurs with a seasonal shift in the meridional location of westerly wind events (WWEs: Harrison and Vecchi 1997). In the 1997–98 El Niño, the southward shift of near-date-line westerly τ^xa was clear (Harrison and Vecchi 1999; Wang and Weisberg 2000; VH06), and it set the timing of the EEqP thermocline shoaling (VH06). It has been suggested that the southward shift of near-date-line τ^xa is fundamentally tied to the annual cycle of insolation, through the nonlinear response of convective anomalies to the location of warmest SST (Harrison and Vecchi 1999; Vecchi and Harrison 2003; VH06; Spencer 2004).

The disappearance and reappearance of the EEqP easterlies in late January/early May 1998 is much more unusual; generally wind anomalies in the EEqP are weak during El Niño (e.g., Wyrtki 1975; Harrison and Larkin 1998; Larkin and Harrison 2002). McPhaden (1999) first noted the likely importance of the January 1998 disappearance and May 1998 return of the EEqP easterlies in the "spectacular finale" of the El Niño, with an explanation for them yet lacking. Independently and using distinct methods, both VH06 and Zhang and McPhaden (2006) show that the unusual disappearance of EEqP easterly τ^x in boreal winter/spring 1998 did, indeed, lead to the extension of the event through boreal spring, and the return of EEqP easterlies led to the abrupt cooling of SST in May.

The mechanisms for the disappearance of the EEqP easterlies remain unclear; the author is aware of no hypothesis other than that of VH06 for their disappearance. Because of the dramatic cooling that followed them, the return of the easterlies in the EEqP in May 1998 has received more attention in the literature than the equally unusual disappearance of the easterlies in late January 1998 (a disappearance that was obviously necessary for their return). Takayabu et al. (1999) and Kiladis and Straub (2003) suggested that internal atmospheric variability [either by the Madden–Julian oscillation (MJO: see Madden and Julian 1994) or by a convectively coupled atmospheric Kelvin wave, respectively)] initiated the return of EEqP easterlies in early May 1998. In the Takayabu et al. (1999) and Kiladis and Straub (2003) scenarios, the stochastic enhancement of easterlies initiated the surface cooling of the EEqP SSTA, terminating the El Niño and returning the normal southeasterly trades. Alternatively Picaut et al. (2002) argue, based on an extensive analysis of oceanic and atmospheric data, that the cooling of the EEqP SSTA resulted from internal oceanic mechanisms, and the return of the EEqP easterlies was driven by the return of cold SSTA. However, VH06 show that the May 1998 cooling of EEqP SSTA resulted from atmospheric forcing, rather than internal oceanic processes. It should also be noted that neither of these suggested mechanisms explains the observed disappearance of the easterlies in late January 1998.

VH06 suggest another interpretation, which addresses both the disappearance and return of the easterlies: the warmest EEqP SST moved onto (north of) the equator beginning late January (late April), resulting in the development (northward retreat) of an equatorial intertropical convergence zone (ITCZ) that removed (returned) the easterlies to the EEqP (see Fig. 9 in VH06). The mechanism proposed by VH06 involves fundamentally meridional, nonlinear, and deterministic changes in atmospheric convection, tied to the annual cycle of insolation and extreme El Niño SST anomalies.

In the rest of this manuscript, the role of particular aspects of the observed SST field in driving the aforementioned atmospheric changes in the end phases of the 1997–98 El Niño event is explored using a series of AGCM experiments. The paper is structured as follows: section 2 describes the atmospheric model and the AGCM experiments, section 3 describes the results of the experiments, and section 4 presents a summary and discussion of the results.

2. AGCM description

a. Model description

The latest version of the NOAA Geophysical Fluid Dynamics Laboratory (GFDL) global atmospheric general circulation model/land model (known as AM2–LM2) was used as the principal tool for the work described here. This model is the atmospheric and land component of the GFDL Coupled Model 2.0 (see Delworth et al. 2006; Gnanadesikan et al. 2006; Wittenberg et al. 2006; Stouffer et al. 2006; Song et al. 2006). The model configuration and its basic climate characteristics are described in GFDL Global Atmospheric Model Development Team (2004, henceforth GAMDT04); the specific configuration used here is referred to as AM2p12b. The atmospheric model has a hydrostatic, finite-difference dynamical core (on a staggered Arakawa B grid) with a hybrid vertical coordinatesigma surfaces below 250 hPa and pressure surfaces aloft. The model resolution is 2° latitude × 2.5° longitude with 24 levels in the vertical. The convective scheme is a Relaxed Arakawa–Schubert scheme (see Moorthi and Suarez 1992), with convective momentum transport. The model has an interactive land model—known as LM2—with specified soil and vegetation types. The reader is referred to GAMDT04 for a more complete discussion of the model physics.

b. Experimental design

1) CONTROL EXPERIMENT

The Control experiment is a 10-member ensemble of 54-yr runs (1950–2003) forced by the global monthly 1° × 1° SST and sea ice data prepared by J. Hurrell (2003, personal communication, provided to GFDL) at the National Center for Atmospheric Research (NCAR). Each ensemble member is started from slightly different initial atmospheric conditions in January 1950. The basic climate of this experiment is described in GAMDT04. Generally the atmospheric circulation over the tropical Pacific, its relationship to El Niño, and the ENSO teleconnections to midlatitudes are well represented by this model (see GAMDT04; Wittenberg et al. 2006; Vecchi et al. 2006).

The focus of the analysis described in this manuscript is the termination of the 1997–98 El Niño. Figure 1 compares the evolution of the near-equatorial Pacific τ^x and τ^xa through the 1997–98 El Niño from the control AGCM run with that from the European Centre for Medium-Range Weather Forecasts (ECMWF) Re-Analysis (ERA-40). Shown is the evolution of both the ensemble mean and a representative ensemble member; the evolution of this particular ensemble member is similar to that of other ensemble members. Anomalies are computed for the Control experiment from the model's 1950–2003 monthly climatology, and for ECMWF using its 1957–2002 monthly climatology. As is evident in Fig. 1, the model is able to reproduce many of the features for the τ^x evolution seen in the ECMWF reanalysis; the character of the evolution of the near-equatorial precipitation variability also agrees with available observations (not shown).

The strong west Pacific westerly τ^xa at the onset of the El Niño is evident in the model, as is the central Pacific westerly τ^xa through the height of the event. In both ECMWF and in the individual ensemble members there is considerable subseasonal variability, with the anomalous westerlies appearing as a series of westerly wind events (WWEs). Enhanced occurrence of WWEs is a characteristic feature of the onset and height of El Niño events (Harrison and Giese 1991; Harrison and Vecchi 1997; Vecchi and Harrison 2000), and they have been shown to lead to substantial warming of the EEqP (Giese and Harrison 1991; Vecchi and Harrison 2000; Lengaigne et al. 2004; Vecchi et al. 2006). The net enhancement of WWE activity through the height of the 1997–98 El Niño was well represented by the AGCM driven by the observed monthly mean SST; the enhancement of WWE activity—in this model framework—did not result from internal atmospheric variability, but was the deterministic response of the atmosphere to the underlying SST (Vecchi et al. 2006).

The principal features of the observed equatorial Pacific τ^x and τ^xa evolution through the end of the 1997–98 El Niño are reproduced by the AGCM forced by observed monthly mean SSTs. The reduction in the strength of central Pacific near-equatorial westerlies in late 1997 is evident in every ensemble member, as is the reduction in the easterly τ^x over the EEqP beginning in late January. The timing and rapidity of the return of the EEqP easterlies is reproduced well by the model, with every ensemble member showing a return of easterlies occurring in the first weeks of May 1998. The changes in the meridional structure of the τ^x field noted by VH06 are well represented within the Control experiment.

2) PERTURBATION EXPERIMENTS

A series of perturbation experiments was performed to test the relative role of changes in the climatology of SST and in the SSTA in producing the meridional changes in the τ^x field at the end of the 1997–98 El Niño. The principal concept behind the experiments was to separate the observed SST into two parts: monthly long-term climatology and monthly anomalies. Then, pairs of experiment ensembles were run by either

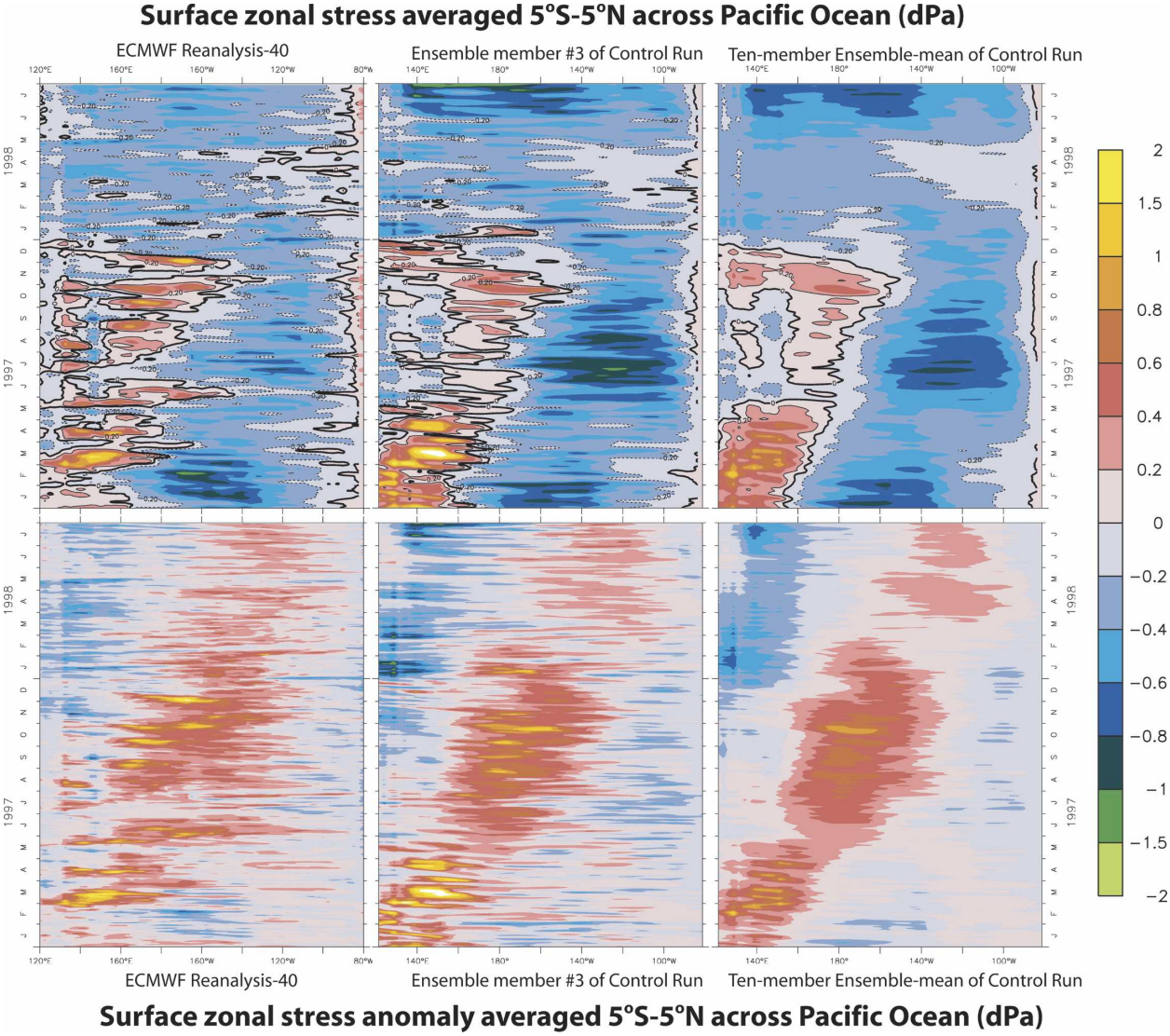

FIG. 1. Time–longitude evolution of the 5-day smoothed Pacific 5°S–5°N (top) τ^x and (bottom) τ^xa from an observational analysis and the Control AGCM experiment, through the 1997–98 El Niño event. (left) The evolution from the ERA-40 dataset, (middle) the evolution from one ensemble member, and (right) the evolution from the 10-member ensemble mean. The key is the same for all panels, and the units are dPa. In the upper panels the {−0.2, 0, 0.2} dPa levels are contoured.

"freezing" the anomalies at the value for a given month (allowing the monthly climatology to vary) or by freezing the climatology at the value for a given month (allowing the monthly anomalies to vary as observed); the AGCM was forced with the total SST (anomaly plus climatology). This method allows assessment of the relative impact of climatological and anomalous SST changes on changes to atmospheric circulation observed after the freeze of the anomalies/climatology.

The principal changes in atmospheric conditions of interest here occurred in mid-November 1997 (southward shift of near-date-line westerly τ^xa), late January 1998 (reduction of EEqP easterlies), and early May 1998 (return of EEqP easterlies). Two pairs of perturbation experiments were run: one pair freezing SST anomalies/climatology in September 1997 (prior to the November 1997 and January 1998 wind changes) and one pair freezing SST anomalies/climatology in March 1998 (prior to the May 1998 return of easterlies).

The perturbation experiments started in September 1997 were named HANOM_SEP97 (for hold anomalies from September 1997) and HCLIM_SEP97 (hold climatology from September 1997). In experiment HANOM_SEP97 the SST anomalies were held fixed at

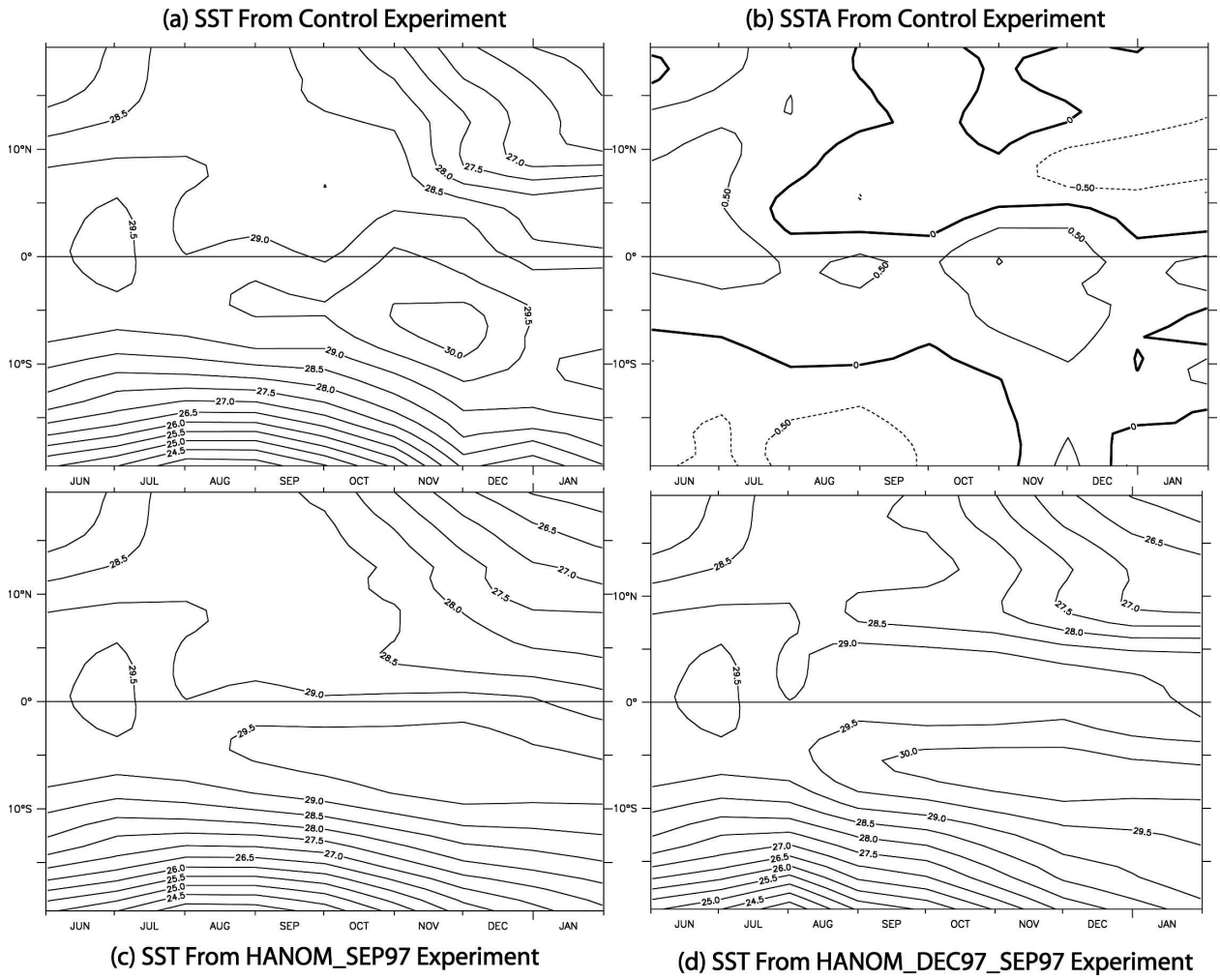

FIG. 2. Time–latitude evolution of near-date-line SST used in the Control and two perturbation AGCM experiments. Monthly mean, 160°E–160°W averaged: (a) SST used to drive Control experiment, (b) SSTA from Control experiment, (c) SST used in HANOM_SEP97 experiment, and (d) SST used in HANOM_DEC97_AUG97 experiment. See text for description of experiment. Units are °C; contour interval is 0.5°C.

their September 1997 values and in experiment HCLIM_SEP97 the SST climatology was held fixed at its September value and the observed SSTA field was added to it. Ten ensemble members were run for each experiment starting from the 1 September 1997 conditions of each of the Control experiment ensemble members. A second experiment pair was named in an analogous manner: HANOM_MAR98 and HCLIM_MAR98. Ten-member ensembles were run for each of these experiments, starting from the 1 March 1998 conditions of each of the Control experiment ensemble members.

In addition another 10-member ensemble of experiments was run to test the impact that the climatological SST had on the atmospheric response to the SSTA changes between September 1997 and December 1997. In this experiment the December 1997 SST anomalies were held beginning August 1997 and climatological SST was allowed to vary. This experiment was named HANOM_DEC97_AUG97.

3. Results

a. Central Pacific changes

In this section, impacts of SST changes on the southward shift of near-date-line τ^xa at the end of 1997 are explored. Figure 2 shows the observed near-date-line SST (Fig. 2a) and SSTA (Fig. 2b) through the end of the event and the SST used in experiments HANOM_SEP97 (Fig. 2c) and HANOM_DEC97_AUG97 (Fig. 2d). Notice in Fig. 2a that there was a shift of the warmest near-date-line SSTs from being centered about the equator to being centered south of the equator toward the end of

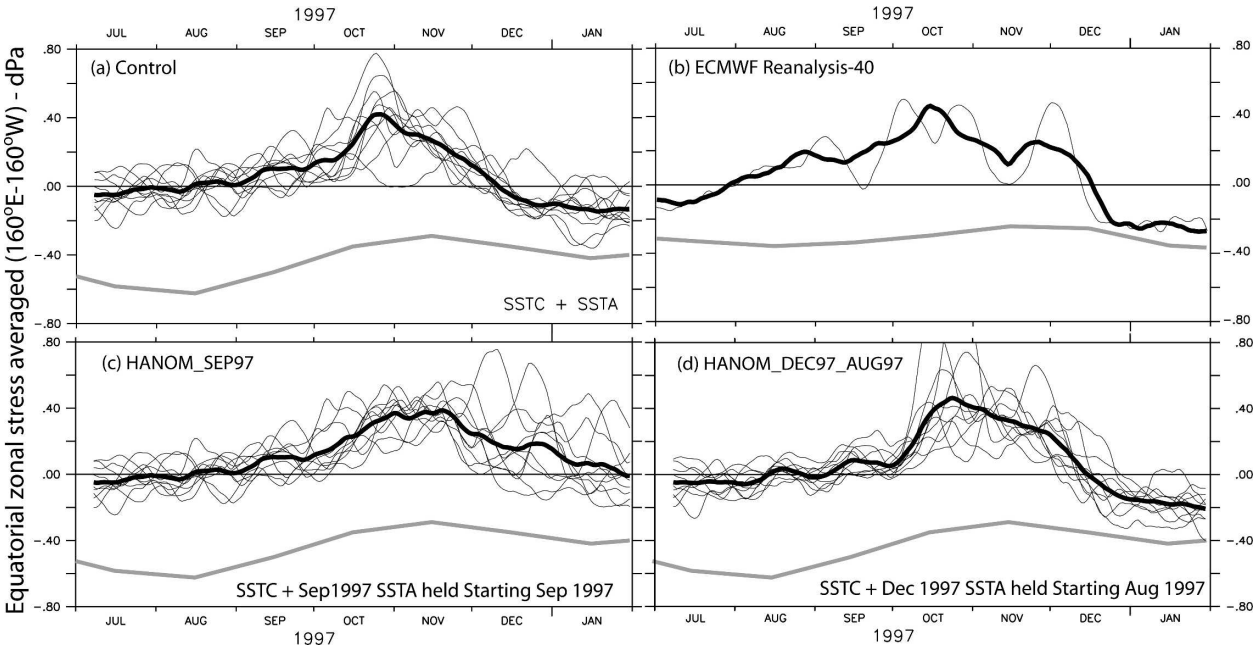

FIG. 3. Time series of near-date-line (160°E–160°W average) equatorial τ^x through the height of the 1997–98 El Niño from the ERA-40, the AGCM Control experiment, and two AGCM perturbation experiments. Shown is the evolution from (a) Control experiment, (b) ERA-40, (c) HANOM_SEP97, and (d) HANOM_DEC97_AUG97; see section 2 for a description of the experiments. For each AGCM experiment thin black lines show the evolution of each of the 10 ensemble members, the thick black line shows the evolution of the 10-member ensemble mean for each experiment (data are smoothed using a 15-day centered mean), and the gray line shows the climatological monthly mean. For ERA-40 the thin black line shows the 15-day smoothed data, the dark black line shows the 31-day smoothed data, and the gray line shows monthly climatology. Units are dPa; positive values indicate westerly τ^x.

1997; this shift arises principally because of the seasonal movement of warmest SSTs. However, there is also a meridional shift in the SSTA field, with warmest SSTA north of the equator in boreal summer and south of the equator in boreal winter (Fig. 2b). This meridional shift in both SSTA and climatological SST results in a stronger hemispheric asymmetry in the forcing for both the Control experiment and HANOM_DEC97_AUG97 than in experiment HANOM_SEP97.

The evolution of near-date-line τ^xa and outgoing longwave radiation (OLR: a proxy for atmospheric convection) from the Control experiment (Figs. 3a, 4a) compares well with that observed [Figs. 3b, 4b; data available online from NOAA's Climate Diagnostics Center (CDC) Web site at http://cdc.noaa.gov/].[1] Each of the 10 ensemble members of the AGCM hindcast exhibits a weakening of the equatorial τ^xa starting November 1997 (Fig. 3a), resulting from a southward shift of the near-date-line τ^xa and convection (Fig. 4a). The southward shift is clear in the ensemble-mean evolution and in that of each ensemble member (not shown), and thus represents the deterministic atmospheric response to the total SST field.

The southward shift of τ^xa occurred at a time when both the meridional structure of the near-date-line climatological SST and SSTA field was changing (see Fig. 2), both of which contributed to the warmest total near-date-line SST being south of the equator (see Fig. 2a). The perturbation AGCM experiment HANOM_SEP97 (Figs. 3c and 4c) indicates that a large part of the southward shift of τ^xa and equatorial westerly τ^xa reduction can be understood in terms of the atmospheric response to the climatological shift in warmest SST. However, the total equatorial τ^xa changes in the Control experiment are larger than those in HANOM_SEP97: changes in SSTA between September and December 1997 also played a significant role. In particular, SSTA cooled in the Northern Hemisphere and warmed in the Southern Hemisphere between September and December 1997 (Fig. 2b); this meridional dipole in SSTA enhanced the meridional migration of warmest SST present in climatology.

The response to the change in SSTA between September 1997 and December 1997 is significantly non-

[1] The OLR data used here is from the NOAA daily interpolated 2.5° × 2.5° OLR dataset.

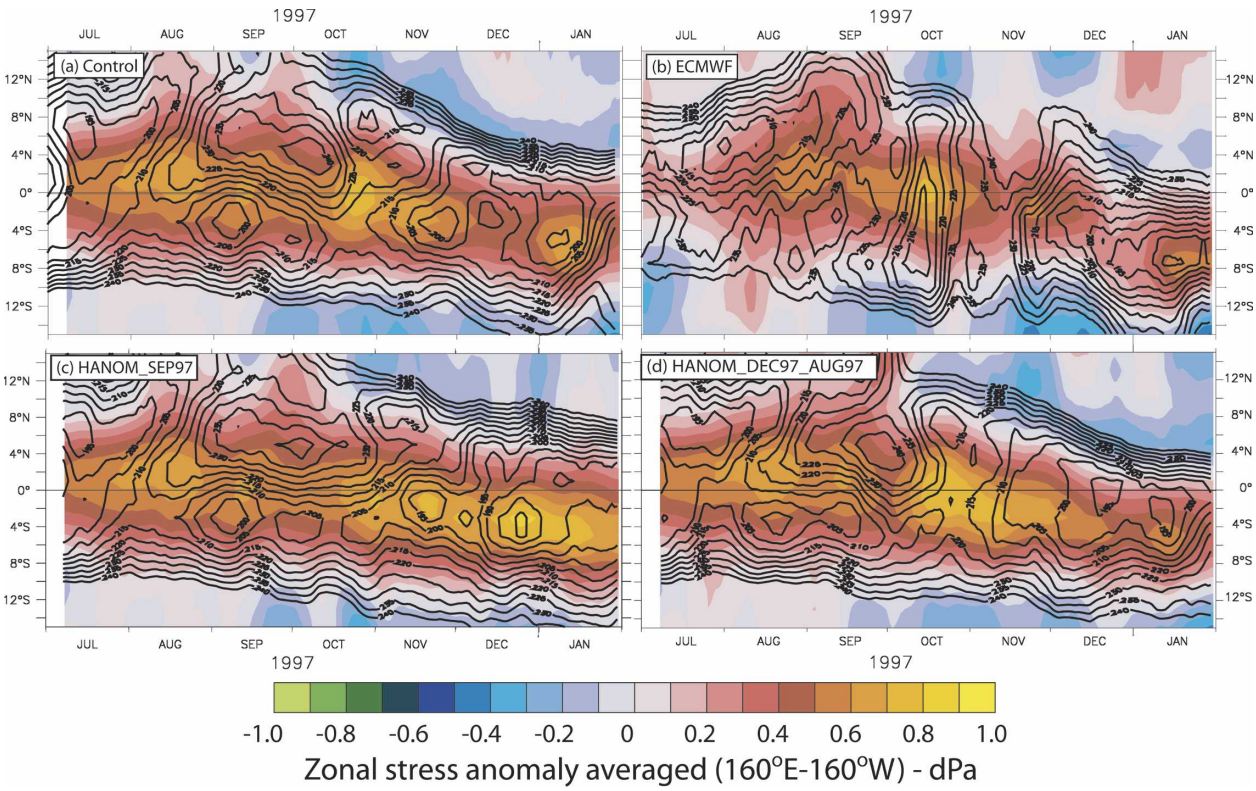

FIG. 4. Time–latitude evolution of the ensemble-mean evolution of tropical near-date-line (160°E–160°W average) τ^xa (shaded) and low OLR (contoured) through the height of the 1997–98 El Niño. Shown is the evolution from (a) 10-member ensemble mean of the Control experiment, (b) observational estimates (τ^x from ERA-40; OLR from the NOAA interpolated OLR product), (c) 10-member ensemble mean of HANOM_SEP97, and (d) 10-member ensemble mean of HANOM_DEC97_AUG97; see section 2b for a description of the experiments. AGCM τ^x data is smoothed using a 15-day centered mean, and ECMWF data is smoothed using a 31-day centered mean; OLR data is smoothed using a 15-day centered mean. Units for τ^x are dPa; positive values indicate westerly τ^x. Units for OLR are W m^{-2}; values less than 240 W m^{-2} are contoured at a 10 W m^{-2} interval.

linear. The December 1997 SSTA enhances the meridional shift in near-date-line westerlies that is evident in the HANOM_SEP97 experiment. However, there is negligible difference in the τ^xa evolution of the Control and HANOM_DEC97_AUG97 experiments throughout the period shown in Figs. 3 and 4. The impact of the December 1997 SSTA was moderated by climatological SST changes: only beginning in December 1997 is there a large difference between HANOM_SEP97 and HANOM_DEC97_AUG97.

b. *East Pacific changes*

In this section, the roles of SST changes on the disappearance of EEqP easterly winds in late January 1998 and their reappearance in early May 1998 are explored. Figure 5 shows the time–latitude evolution of the observed eastern tropical Pacific SST (Fig. 5a) and SSTA (Fig. 5b) through the end of the event and that of the SST used to force the perturbation experiments (Figs. 5c–f). The forcing for HANOM_SEP97 and the Control has the warmest SST in the eastern tropical Pacific moving over the equator in January 1998, while that for HCLIM_SEP97 has its warmest SST north of the equator throughout the whole period. The forcing for HANOM_MAR98 and the Control has the warmest SSTs move north of the equator in May 1998 but lacks the strong cooling of surface waters in May 1998 (Fig. 5e). Meanwhile, the forcing for experiment HCLIM_MAR98 includes the strong cooling in May 1998 but has its warmest SSTs symmetric about the equator (Fig. 5f).

In both observations and the Control experiment, the disappearance of the EEqP easterlies began in late January 1998, and their sudden reappearance was in early May 1998 (Figs. 6a–b). Both of these features are evident in every ensemble member of the Control experiment; thus they represent the deterministic response of the AGCM to the total SST forcing. Early 1998 was characterized by the development of an equatorially centered ITCZ throughout the period in which

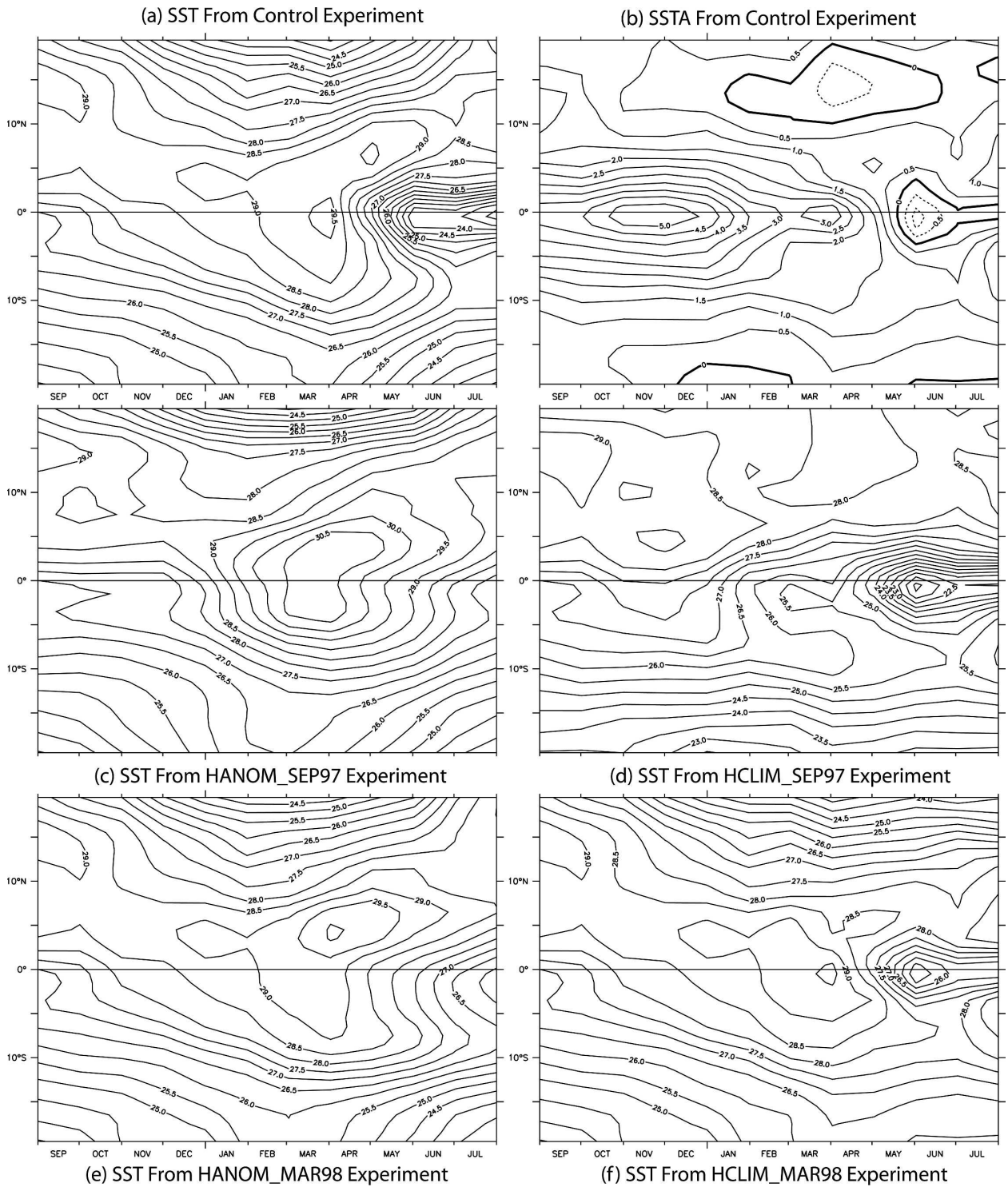

FIG. 5. As in Fig. 2 but for the east Pacific (120°–105°W) SST forcing for the Control and four perturbation AGCM experiments: (a) SST used to drive Control experiment, (b) SSTA from Control experiment, (c) SST used in HANOM_SEP97 experiment, (d) SST used in HCLIM_SEP97 experiment, (e) SST used in HANOM_MAR98 experiment, and (f) SST used in HCLIM_MAR98 experiment. See text for description of experiments. Units are °C; contour interval is 0.5°C.

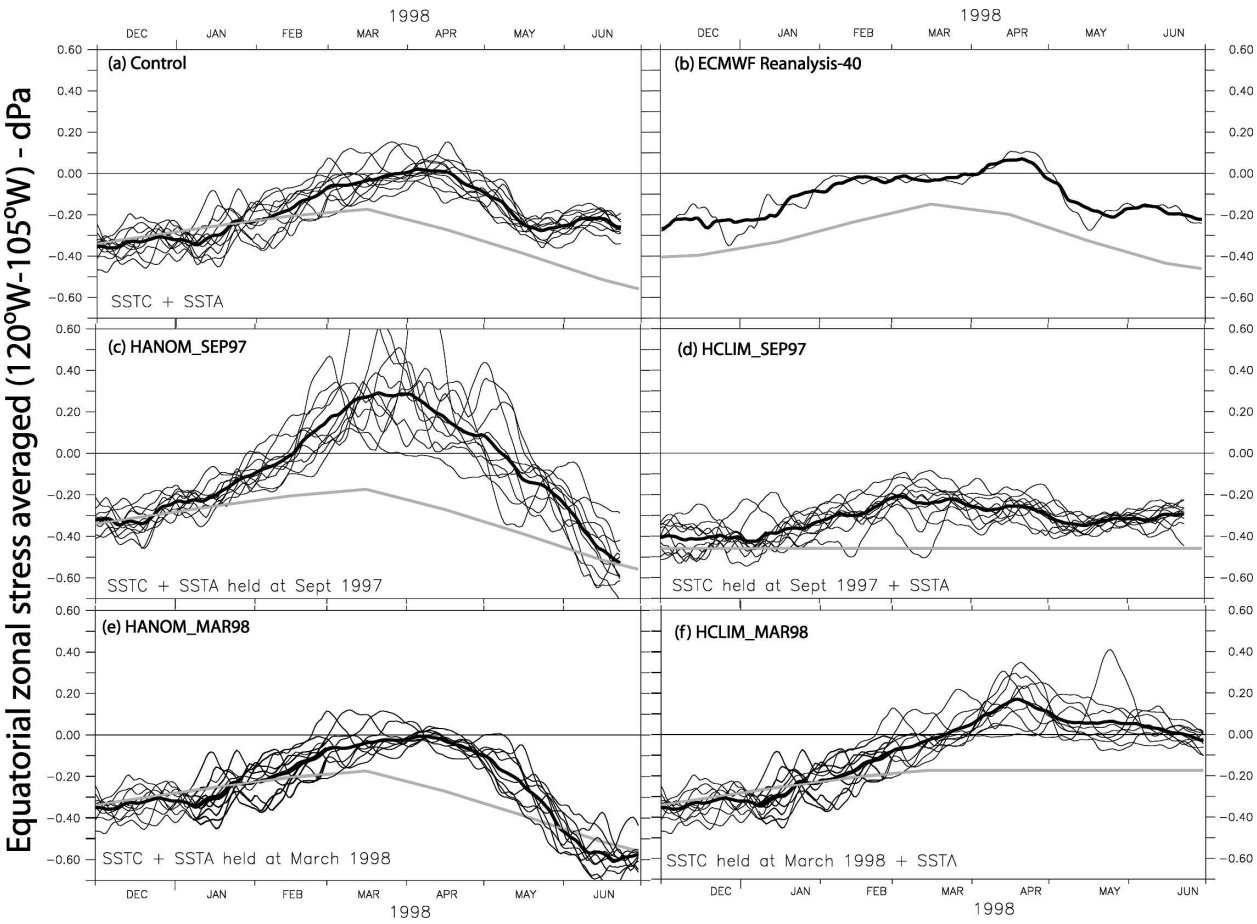

FIG. 6. Similar to Fig. 3 but for the eastern Pacific (120°–105°W average). Shown is the evolution from (a) Control experiments, (b) ERA-40, (c) HANOM_SEP97, (d) HCLIM_SEP97, (e) HANOM_MAR98, and (f) HCLIM_MAR98; see text for description of experiments. Units are dPa; positive values indicate westerly τ^x.

the easterlies disappeared, evident in the OLR evolution in observations (Fig. 7a). In early 1998, the Control AGCM experiment (Fig. 7b) has eastern Pacific atmospheric convection concentrated on the equator: however, it shows a tendency for a "double ITCZ" during early 1998, with lowest OLR not directly on the equator. This tendency for a double rather than equatorially centered ITCZ may be why the AGCM winds are slightly more easterly than in observations (Fig. 6).

Perturbation experiments HCLIM_SEP97 and HANOM_SEP97 serve to explore the extent to which the disappearance of EEqP easterlies resulted from the preexisting strong SSTA field and the climatological warming of the EEqP in boreal spring. The disappearance of EEqP easterly τ^x in January 1997 occurs in the HANOM_SEP97 (Fig. 6c), while it is not evident in the HCLIM_SEP97 (Fig. 6d). The warmest SSTs in the HANOM_SEP97 experiment move onto the equator in January 1998, while in HCLIM_SEP97 they remain north of the equator even though the equatorial SSTA increases between September 1997 and December 1997 (Fig. 5). The AGCM results suggest that the disappearance of the EEqP easterlies resulted from the warmest eastern tropical Pacific SST being near the equator in early 1998.

Perturbation experiments HCLIM_MAR98 and HANOM_MAR98 serve to explore the extent to which the return of easterly EEqP τ^x was related to the sudden cooling in May 1998 and the extent to which it resulted from the seasonal warming in the Northern Hemisphere. In experiment HCLIM_MAR98, which includes the sudden cooling of SSTA in May 1998, there was no return of easterlies (Fig. 6f). Meanwhile, in the HANOM_MAR98 experiment suite, the equatorial easterlies return in May 1998 (Fig. 6e), even though the SST anomalies remain quite warm (Fig. 5b). In this AGCM the return of EEqP easterlies in May 1998 was driven by the seasonal movement of warmest

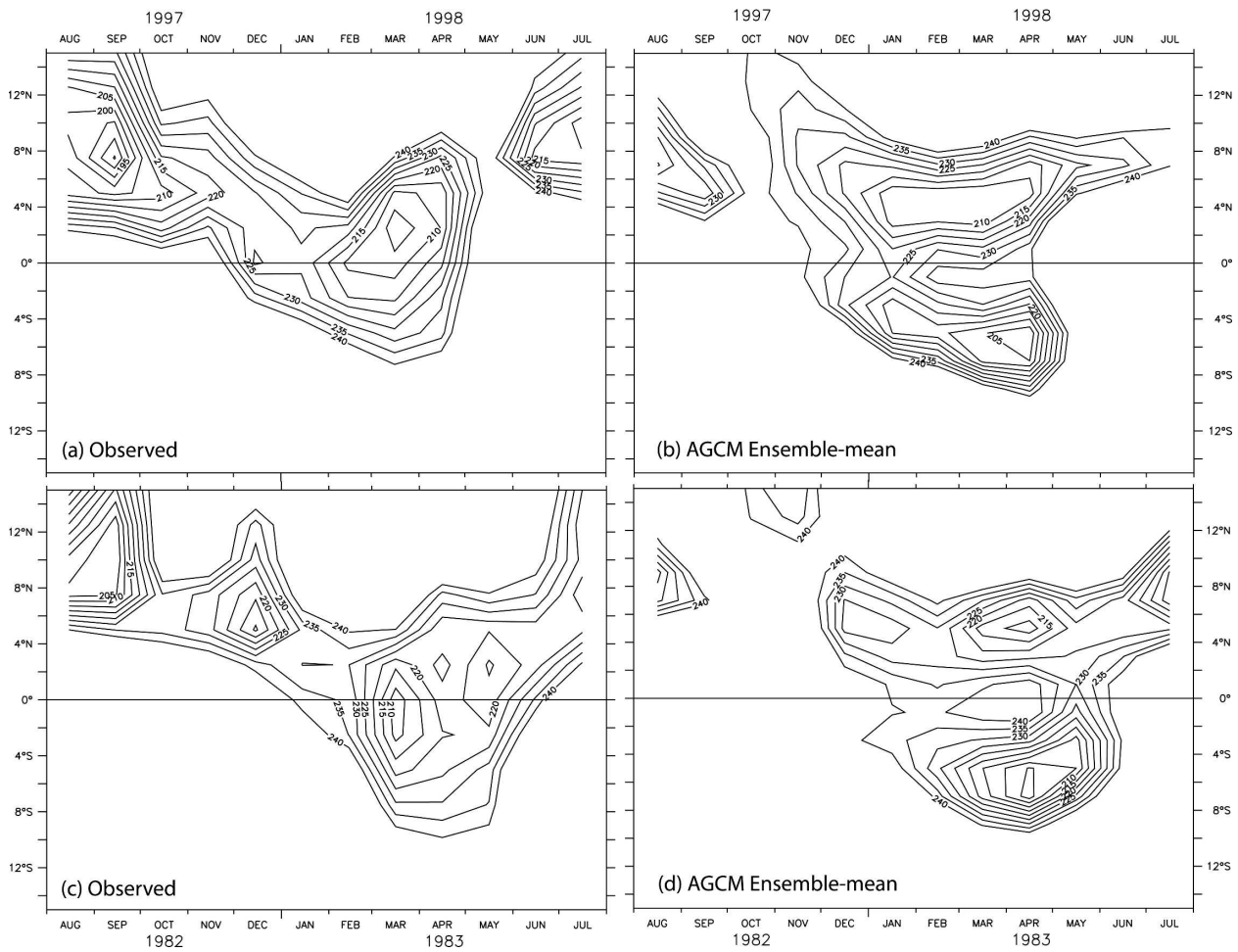

FIG. 7. Time–latitude evolution of monthly mean tropical eastern Pacific (120°–105°W average) OLR from NOAA interpolated observational dataset and the 10-member ensemble mean of the Control AGCM experiment. Shown is the (a) observed and (b) AGCM July 1996–June 1999 evolution. Units for OLR are W m^{-2}; values less than 240 W m^{-2} are contoured at a 5 W m^{-2} interval.

SSTs north of the equator at the end of boreal spring and coincided with a northward retreat of the ITCZ.

The EEqP surface easterlies after May 1998 are stronger in experiment HANOM_MAR98 (Fig. 6e) than in the Control experiment (Fig. 6a), suggesting that the SSTA cooling in May 1998 resulted in weaker surface easterlies than those that would have been present if the SSTA had not cooled in response to the easterlies. This apparently counterintuitive feature of the experiments appears related to the destabilization of the EEqP atmospheric boundary layer in the presence of warmer SSTs in the perturbation experiment (HANOM_MAR98). The boundary layer in HANOM_MAR98 is deeper than in the Control experiment (not shown); and the EEqP zonal winds, averaged from 1000 to 850 hPa, are comparable in both experiments. This relationship between cold SST and surface τ^x weakening is a ubiquitous feature over the oceans, on many time scales (e.g., Wallace et al. 1989; Chelton et al. 2004; Xie 2004).

c. *Differences between moderate and extreme El Niño events*

This section explores the extent to which the peculiar evolution at the end of the 1997–98 El Niño could be expected to be a general feature of extreme El Niño events. In 1982–83 another extreme El Niño event occurred, the termination of which was comparable to that of 1997/98 (e.g., Philander and Seigel 1985; Harrison et al. 1990; Zhang and McPhaden 2006); EEqP easterlies disappeared in early 1983 and returned suddenly in June 1983. The lower panels of Fig. 8 indicate that the meridional evolution of east Pacific OLR in 1982–83 was also similar to that of 1997–98, with the development of equatorially concentrated convection in early 1983. The disappearance of EEqP easterlies in

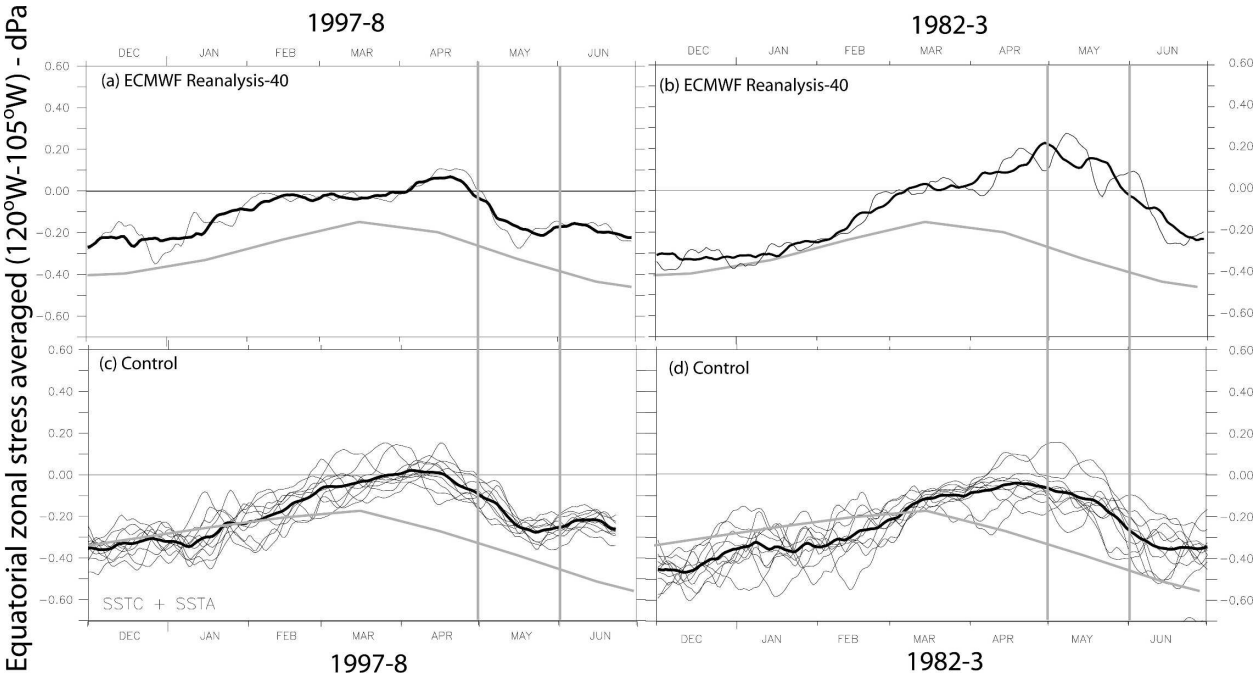

FIG. 8. Time series of eastern Pacific (120°–105°W average) equatorial τ^x through the height of (left) the 1997–98 El Niño and (right) the 1982–83 El Niño from the ERA-40, the AGCM Control experiment, and two AGCM perturbation experiments. Shown is the evolution from (a)–(b) ERA-40 and (c)–(d) Control. Units are dPa; positive values indicate westerly τ^x. Gray line shows climatological τ^x.

early 1983 and their return in June 1983 was represented in the AGCM, and the timing of the disappearance/return of the easterlies in each El Niño is coincident with the meridional changes in OLR—easterlies disappear (return) as convection is centered about (moves north of) the equator (Fig. 8).

Figure 9 shows how unusual the evolution of east Pacific OLR in these two El Niño events has been, in both observations and the AGCM. Only in boreal spring at the height of the two extreme El Niño events (1982–83 and 1997–98) is an equatorially centered region of low OLR evident in the eastern Pacific. Throughout practically the entire record, atmospheric convection remains centered around 10°N; not even in the moderate El Niño events of 1987–88, 1991–92, and 2002–03 does convection straddle the equator. In both of the extreme El Niño events EEqP SSTA was large enough that, in boreal late winter/spring, the warmest total SST was centered on the equator. Could the disappearance of EEqP easterlies, development of an equatorial ITCZ, and delayed termination of El Niño be general features of extreme events?

A series of AGCM experiments explores the response of EEqP convection and winds to idealized "El Niño" forcing of weak (1°C) and strong (4°C) amplitudes. Two 10-member AGCM ensembles are run, each forced using monthly climatological SST plus an idealized El Niño SSTA field with the same structure, but different amplitude. The structure of the time-invariant idealized SSTA field is shown in Fig. 8, and its analytical form is

$$\mathrm{SSTA}(x, y) = A \exp[-(y/6)^2] \times \langle 0.5\{\tanh[(x - 180)/20] + 1\}\rangle,$$

where A is the amplitude of the SSTA forcing (1°C for the weak, and 4°C for the strong El Niño), and x and y are the longitude and latitude, in degrees. In both perturbation experiments the east Pacific SST anomalies are equatorially centered, however the meridional location of the warmest total east Pacific SST depends on SSTA amplitude and season. Only in boreal late winter/early spring of the strong El Niño experiment (4°C anomaly) are the warmest east Pacific SSTs centered about the equator; otherwise the warmest SSTs are north of the equator (~5°–10°N).

Figure 10 shows the time–latitude evolution of eastern tropical Pacific OLR from the Control run monthly climatology and from the 10-member ensemble mean of each of the two idealized El Niño experiments. In each perturbation experiment there is a strengthening of atmospheric convection relative to the AGCM climatology, which is most pronounced in boreal spring. However, the meridional structure of the boreal spring-

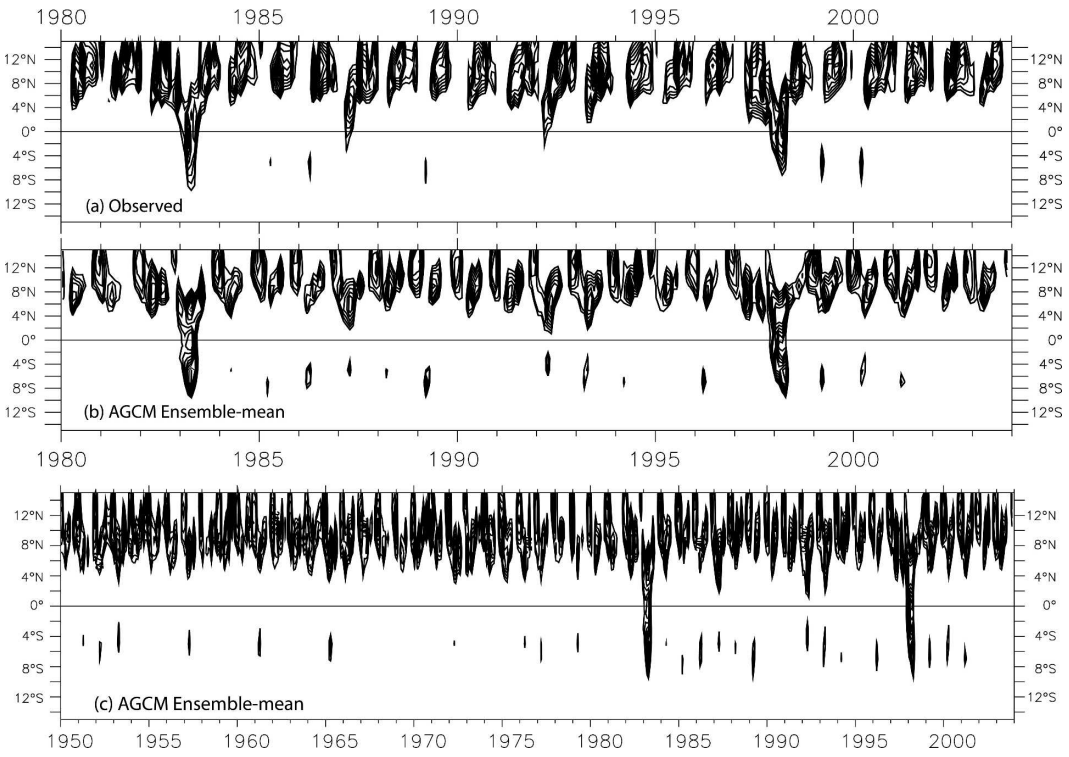

FIG. 9. As in Fig. 7 but for the (a) observed, (b) AGCM 1980–2003 evolution, and (c) AGCM 1950–2003 evolution.

time OLR in the strong idealized El Niño experiment differs from both the Control climatology and the weak El Niño by showing a clear development of an equatorial ITCZ; the equatorial ITCZ is evident in all 10 ensemble members of the strong idealized El Niño experiment. The equatorial ITCZ develops in the strong idealized El Niño experiment at the time when the warmest SSTs are close to the equator and retreats north of the equator as the warmest SSTs do.

The evolution of EEqP zonal wind stress during the strong El Niño experiments is also distinctive (Fig. 11).

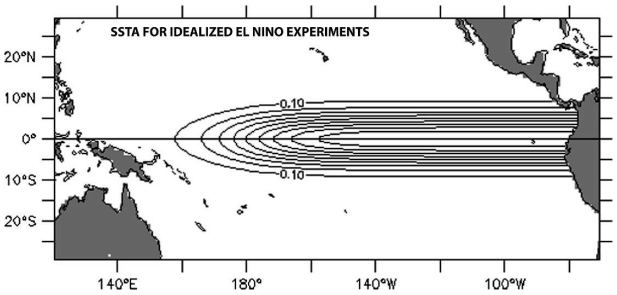

FIG. 10. Spatial structure of the time-invariant SST anomaly field used in the idealized El Niño experiments. This SSTA field is multiplied by a scale factor of {1°, 2°, 4°C} and added to the monthly climatology.

The surface zonal wind stress anomaly for the 1°C idealized El Niño experiments are generally weak, with the absolute wind stress always remaining easterly. However, the strong El Niño experiment shows significant anomalies with the equatorial easterlies disappearing in late boreal spring. The disappearance of the easterlies is coincident with the development of the equatorial ITCZ, and the easterlies return as the ITCZ retreats north of the equator.

d. Differences between two extreme El Niño events

Though the disappearance of EEqP easterlies and the development of an equatorial ITCZ are features to be expected of extreme El Niño events, Figs. 7 and 8 show that there was a difference in the timing of the northward retreat of the equatorial ITCZ between the 1982–83 and 1997–98 El Niño events. In the 1997–98 El Niño event the ITCZ moved north of the equator in late April/early May 1998; whereas in the 1982–83 El Niño the ITCZ did not return north of the equator until mid-June 1983. Having argued that a deterministic (in the atmosphere-only context), seasonally phase-locked process is fundamental to the extension and sudden termination of extreme El Niño events, this difference in timing presents a feature worth discussion. Two gen-

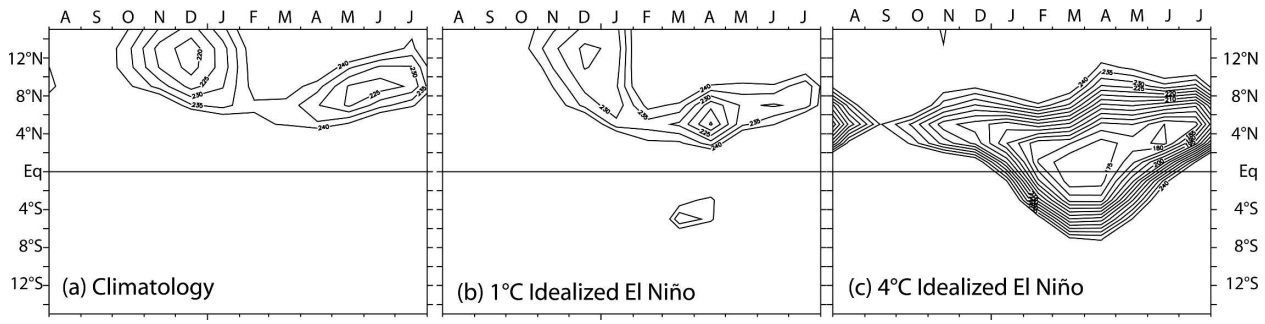

FIG. 11. Time–latitude evolution of monthly mean eastern tropical Pacific OLR for (a) the AGCM Control experiment climatology, and the 10-member ensemble means for the (b) 1°C and (c) 4°C idealized El Niño AGCM experiments. Units are W m^{-2}. OLR is averaged between 120° and 105°W, and only values lower than 240 W m^{-2} are contoured at 5 W m^{-2} intervals.

eral explanations present themselves: 1) stochastic atmospheric variability leads to the interevent differences and 2), because of the fundamentally nonlinearity of the mechanism, differences in SSTA impacted the timing of the atmospheric changes.

The impact of internal atmospheric variability on the timing of the return of the easterlies in the EEqP can be seen quite clearly in Figs. 6, 8, and 11. The timing of the easterly return is slightly different in each ensemble member of the AGCM experiments in which they disappear (Control in 1998 and 1983: Figs. 6a, 8b–d; HANOM_SEP97: Fig. 6c; HANOM_MAR98: Fig. 6e; the 4°C idealized El Niño: Fig. 11). The dispersion about the time of easterly return in the ensemble mean is roughly ±10 days. If the AGCM estimate of internal atmospheric variability is correct, then the atmosphere limits the predictability of the return of easterlies at the end of an extreme El Niño event by the order of a few weeks. However, the difference between the easterly return in 1998 and in 1983 is over 30 days, beyond the range that one can expect given the AGCM estimate of internal atmospheric variability: in none of the ensemble members in the Control experiment or experiment HANOM_MAR98 was the return of easterlies in June 1998, and in none of the ensemble members of the Control experiment was the return of easterlies in early May 1983.

Can the differences between the timing of the return of the easterlies in the 1997–98 and 1982–83 El Niño events be understood in terms of the deterministic response of the atmosphere to SST? Figures 11c and 11d show the time series evolution of the EEqP τ^x through the end of the two extreme El Niño events for the Control experiment. The difference in timing of the return of the easterlies is evident in the ensemble mean of the AGCM simulations of the two El Niño events: the ensemble-mean return of easterlies began in late April for 1998 and late May for 1983. Thus, to a large extent, the differences in the timing of the return of easterly EEqP τ^x in these two extreme El Niño events can be understood in terms of the nonlinear deterministic response to different SST fields.

There are differences between the east Pacific SSTA in early 1983 and that in early 1998 that suggest the reason for the different timing of the return of the EEqP easterlies in these two extreme El Niño events (Fig. 12): The meridional structure of the east Pacific SSTA in early 1983 shows a distinct asymmetry, with waters anomalously warmer in the Southern Hemisphere than in the Northern Hemisphere; meanwhile, the east Pacific SSTA in early 1998 shows much more of a symmetric pattern (relative to early 1983, early 1998 is warmer in the Northern Hemisphere and cooler in the Southern Hemisphere). If the timing of the return of the easterlies in these two El Niño events was set by the seasonally driven return of warmest EEqP SSTs to the Northern Hemisphere, this SSTA asymmetry should be of influence. The seasonal warming of the Northern Hemisphere needed to progress further in 1983 than in 1998 to place the warmest total SST north of the equator. In nonlinear regimes, such as the EEqP during extreme El Niño events, details in the SSTA structure have significant influence on the evolution of the system.

4. Summary and discussion

Through a series of experiments with the NOAA/GFDL AM2p12b global atmospheric general circulation model (AGCM: see GAMDT04) the mechanisms controlling surface τ^x changes in the near-equatorial Pacific at the end of the extreme 1997–98 El Niño are explored. The focus of this paper is three features of the equatorial τ^x that set the timing of the termination of the El Niño: (i) a reduction of equatorial near-date-line surface τ^xa beginning November 1997, (ii) the disappearance of the easterly τ^x from the eastern equatorial

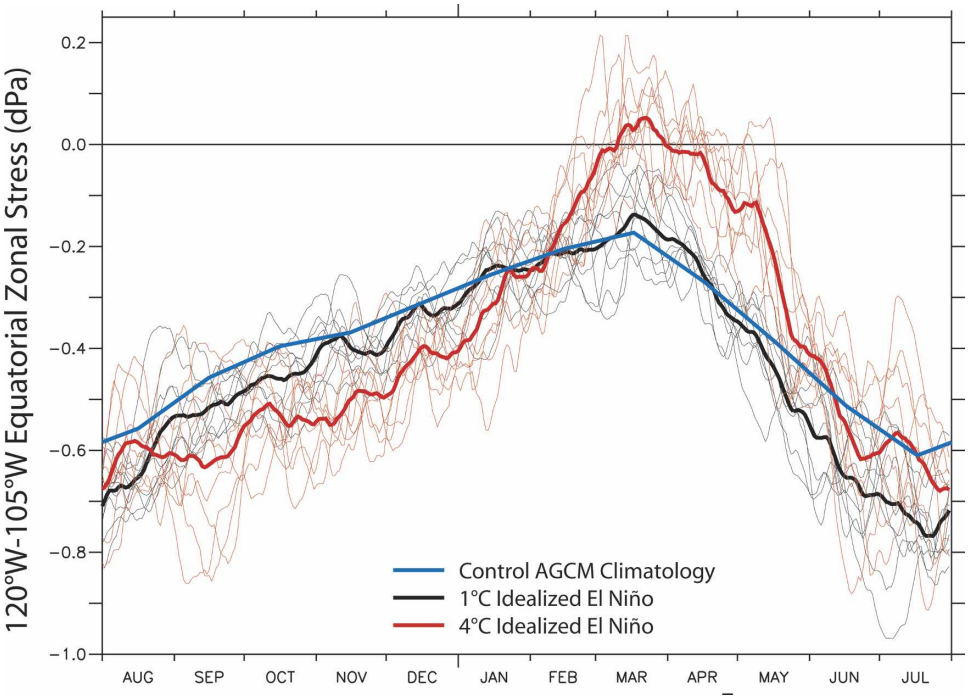

FIG. 12. Time series of the eastern equatorial Pacific zonal wind stress for the AGCM Control climatology and for the idealized El Niño experiments. Shown in black is the evolution for the weak (1°C) and in red the for the strong (4°C) idealized El Niño experiments; blue line shows 1950–2000 climatological values. Thin lines indicate the evolution of each ensemble member, and thick lines show the 10-member ensemble mean evolution; units are dPa.

Pacific (EEqP) in February 1998, and (iii) the reappearance of easterly τ^x in the EEqP in May 1998. The AGCM experiments described in this paper indicate that these equatorial τ^x changes were determined by the observed SST field and resulted from atmospheric circulation changes that were fundamentally meridional in character. Many aspects of these τ^x changes were fundamentally controlled by the changes in climatological SST, which modified the atmospheric response to changes in the SSTA field.

The AGCM, forced by the observed monthly mean SST field, is able to reproduce the principal features of the equatorial Pacific surface τ^x and τ^xa evolution through this El Niño (see Fig. 1). Though tangential to the principal focus of this paper, it is quite interesting that the AGCM reproduces the enhancement of westerly wind event (WWE) activity through the onset and development of the El Niño. In this model, the enhancement of WWE variability from the onset to the height of the 1997–98 El Niño represents the deterministic response to the total SST, not internal atmospheric variability. More relevant to the principal focus of this paper was that the timing and amplitude of the equatorial τ^x changes at the end of the El Niño event were well represented in the model.

The reduction of near-date-line τ^xa at the end of 1997 was associated with the southward shift of near-date-line τ^xa, which is a robust boreal winter feature of El Niño events (e.g., Harrison 1987; Harrison and Larkin 1998; Larkin and Harrison 2002). AGCM experiments presented in section 3a indicate that the changes of near-date-line τ^xa at the end of 1997 were driven by changes to the SST field, in particular through the seasonally influenced meridional location of warmest SST. Much of the southward shift could be understood in terms of the AGCM response to changes in the climatological SST, holding SSTA constant at its September 1997 values. Additionally, a significant part of the τ^xa weakening was associated with changes in SSTA between September 1997 and December 1997. However, the response to changes in SSTA is quite nonlinear: the impacts of the December 1997 SSTA are negligible prior to December 1997 (see Fig. 3). Because of the nonlinear relationship between SST and convection, changes in the climatological SST fundamentally alter the response of near-date-line atmospheric conditions to SSTA, leading to a boreal winter reduction of equatorial τ^xa through a southward shift of convection.

The results presented here are consistent with the recent work of Spencer (2004), who finds that the re-

sponse of the Second Hadley Centre Atmospheric Model (HadAM2) to a time-invariant El Niño SSTA field over a monthly varying SST climatology is for a southward shift of near-date-line τ^xa in boreal winter. However, changes in SSTA are also important to the southward shift; a cooling of the Northern Hemisphere west Pacific, as described by Guilyardi et al. (2003), could be part of the forcing for the southward wind shift. The potential influence of meridional changes similar to those in the evolution of an intermediate-complexity coupled model of El Niño was shown by An and Wang (2001). When An and Wang imposed a seasonally varying statistical correction—which includes a seasonally phase-locked southward shift of near-date-line τ^xa—on the Cane–Zebiak (Zebiak and Cane 1987) intermediate coupled model, there was a significant improvement in the timing of the model system's transition from El Niño to La Niña. The southward shift of near-date-line τ^xa represents a physical mechanism for the seasonal dependence of the ocean–atmosphere coupling coefficient that has been used to study the role of interactions between seasonal and interannual variations (e.g., Tziperman et al. 1998); a seasonally dependent coupling coefficient results in both a strong seasonal phase locking of El Niño and irregularity in the system.

The southward shift of near-date-line surface τ^xa is also evident in coupled general circulation models (CGCMs) and appears to control the timing of the termination of El Niño in these model systems (e.g., Vecchi et al. 2004; Lengaigne et al. 2006). Through a series of coupled ocean–atmosphere model experiments, Lengaigne et al. (2006) show that a southward shift of the near-date-line westerly τ^xa during boreal winter, driven by the annual cycle of insolation, is important in setting the thermocline shoaling at the end of El Niño in the Hadley Centre Coupled Atmosphere–OPA Climate Model (HadOPA) coupled system.

Within the model framework presented here, the late January 1998 disappearance and early May 1998 return of the EEqP easterlies was the deterministic response of this AGCM to the observed SST field, associated with the unusual development/northward retreat of an equatorial ITCZ in early 1998 (see section 3b). The AGCM experiments presented here show that changes in the climatological SST field, in the presence of invariant extreme SST anomalies, result in the disappearance/return of EEqP easterlies. The perturbation AGCM experiments establish that the timing of the return of the EEqP easterlies was principally associated with the seasonal meridional movement of the warmest SST, and not an atmospheric response to the strong May 1998 cooling of EEqP SSTA. In fact, the SSTA cooling reduces the surface manifestation of the easterlies by stabilizing the atmospheric boundary layer (see section 3b). Thus, while there is a strong causal link from the return of the easterlies to the SSTA cooling in May 1998 (VH06), it appears that the strong EEqP SSTA cooling in May 1998 was not the principal factor that caused the winds to return the easterly winds.

In 1982–83 another extreme El Niño event occurred, which showed similar evolution to 1997–98 in its termination. Model hindcasts of the event indicate that the Z_{tc} shoaled in early 1983, but SST did not return to normal until surface easterlies returned abruptly in June 1983 (Philander and Seigel 1985; Harrison et al. 1990); the analysis of Zhang and McPhaden (2006) also identify the 1982–83 El Niño event as one whose termination was influenced by the disappearance of EEqP easterlies. Interestingly, examination of the meridional evolution of east Pacific OLR and winds in 1982–83 reveals the development of an equatorial ITCZ at the end of that major El Niño event (Figs. 7 and 9). In the moderate El Niño events the EEqP winds remain easterly (Wyrtki 1975; Harrison and Larkin 1998; Larkin and Harrison 2002; Zhang and McPhaden 2006) and an equatorial ITCZ does not develop (Fig. 9).

A series of AGCM experiments with idealized "El Niño" SSTA indicate that the atmospheric response in the eastern equatorial Pacific is different for weak and for extreme El Niño events (see section 3c). Weak El Niño SSTA forcing induces little change in τ^xa in the eastern equatorial Pacific, with robust easterly trades remaining through the event and no formation of an equatorial ITCZ. Meanwhile, there is a pronounced development of a boreal springtime equatorial ITCZ and disappearance of EEqP easterlies in every experiment forced by extreme idealized El Niño SST anomalies (see Figs. 11–12).

Though a seasonally controlled disappearance/return of EEqP easterlies appears to be an expected characteristic of extreme El Niño events, there are nonnegligible differences in the timing of the return of EEqP easterlies between the 1982–83 and 1997–98 El Niño events (Figs. 7, 8). These differences need to be reconciled with the deterministic framework presented here. One possible explanation is that the difference in the timing of the return of the easterlies between 1982–83 and 1997–98 resulted from stochastic forcing by the atmosphere. The observational results of Takayabu et al. (1999) and Kiladis and Straub (2003) present one possible source of stochastic forcing: the MJO or a convectively coupled atmospheric Kelvin wave. However, the estimate of the dispersion on the time of return of easterlies attributable to internal atmospheric variability in the AGCM used here is not sufficient to explain the

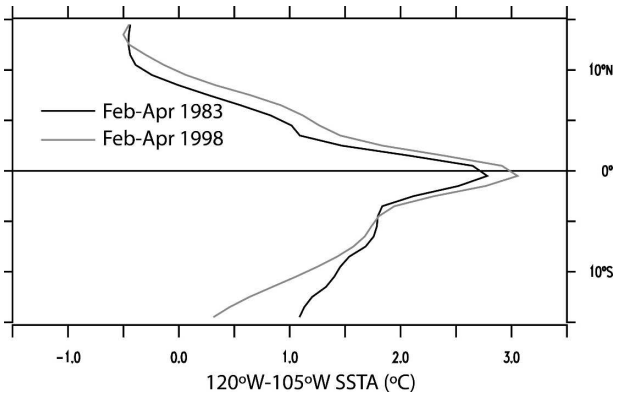

FIG. 13. NOAA optimal interpolation (OI) (Reynolds et al. 2001) sea surface temperature anomalies averaged from 120° to 105°W at the height (February–April) of the 1982–83 (black line) and 1997–98 (gray line) El Niño events.

observed difference in timing between 1982–83 and 1997–98.

Another possible explanation (which does not preclude the influence of stochastic forcing) is that, because of the nonlinear processes involved, differences in the SSTA field between 1982–83 and 1997–98 resulted in different timing of the return of the easterlies. This explanation is supported by the evolution of the 10 ensemble members of the Control experiment in 1982–83 and 1997–98, which showed a consistently different timing in the return of easterlies in each El Niño event. The AGCM forced with 1982–83 SST returned easterlies later in the year than when forced with 1997–98 SST (Fig. 8), in a manner consistent with observations. Differences in the meridional structure of SSTA in these two El Niño events may have resulted in the different timing of the easterly return (Fig. 13); experiments are underway to test this suggestion.

Various facets of a strong interplay between the annual cycle and anomalous El Niño conditions have been discussed in the literature. Seasonal changes in the state of the ocean may impact the instability of the tropical Pacific coupled ocean–atmosphere system (e.g., Xie 1995; Tziperman et al. 1997; Galanti and Tziperman 2000; Galanti et al. 2002). Additionally, seasonal changes in the specified background atmospheric conditions, particularly in background convergence associated with movements of the ITCZ, strongly influence the evolution of El Niño in intermediate coupled models, acting to modify the underlying oscillator mechanism (e.g., Jin et al. 1994; Tziperman et al. 1994; Chang et al. 1994, 1995; Tziperman et al. 1995, 1997, 1998). Changes in the meridional structure of atmospheric anomalies, related to the annual cycle of insolation, appear fundamental in setting the timing of the termination of El Niño (e.g., Harrison and Vecchi 1999; An and Wang 2001; Vecchi and Harrison 2003; VH06; Vecchi et al. 2004; Spencer 2004; Lengaigne et al. 2006).

It has been shown that interactions between interannual and seasonal variations in the tropical Pacific could induce some of the observed irregular behavior of El Niño (e.g., Tziperman et al. 1994; Jin et al. 1994; Chang et al. 1994; Tziperman et al. 1995; Chang et al. 1995). Additionally, the sensitivity of the system to details in the SST anomaly structure can explain some of the differences in the evolution of El Niño events (see section 3d). Thus, one may need not appeal directly to stochastic atmospheric forcing to explain some of the differences between El Niño events—though stochastic forcing may tend to enhance the intrinsically chaotic behavior of the system.

The work presented here suggests that the termination of a strong El Niño involves a considerable degree of nonlinearity. Penland and Sardeshmukh (1995) are able to successfully capture many of the principal features of El Niño through a linear statistical model, which breaks down at the height of extreme El Niño events; the breakdown of the linear model may result from its inability to represent the nonlinear processes involved in the disappearance of EEqP easterlies (and resulting decoupling between ocean surface and subsurface temperature changes).

Many aspects of interannual variability in the tropical Pacific are influenced by the annual cycle. In particular, the termination of El Niño events is strongly controlled by interactions between the annual cycle and anomalous conditions. Thus, better understanding and representation of the impact of the annual cycle of insolation on the interannual variations of the tropical Pacific coupled ocean–atmosphere system may help improve forecasts of El Niño. Models of the tropical coupled ocean–atmosphere system used to study El Niño should either resolve or parameterize these nonlinear interactions.

Acknowledgments. This research was supported by the Visiting Scientist Program at the National Oceanic and Atmospheric Administration/Geophysical Fluid Dynamics Laboratory (NOAA/GFDL), administered by the University Corporation for Atmospheric Research (UCAR). Analysis and graphics are done using freeware package Ferret (http://ferret.wrc.noaa.gov/). I gratefully acknowledge the TAO project office for making the TAO data easily and readily available. The OLR and SST data made easily accessible by NOAA–CDC, Boulder, Colorado, is appreciated. Special thanks to the Global Atmospheric Model Development Team at NOAA/GFDL for the development and tun-

ing of the atmospheric model, and to Rich Gudgel for running the Control experiments. Helpful comments, discussion and suggestions from D. E. Harrison, M. Harrison, S. Ilcane, G. Kiladis, N.-C. "G" Lau, M. McPhaden, A. Rosati, Q. "S" Song, and A. Wittenberg. I am grateful for the insightful comments and suggestions from E. Tzipperman and two anonymous reviewers.

REFERENCES

An, S.-I., and B. Wang, 2001: Mechanisms of locking of the El Niño and La Niña mature phases to boreal winter. *J. Climate,* **14,** 2164–2176.

Barnston, A. G., M. H. Glantz, and Y. He, 1999: Predictive skill of statistical and dynamical climate models in SST forecast during the 1997–98 El Niño episode and the 1998 La Niña onset. *Bull. Amer. Meteor. Soc.,* **80,** 217–243.

Boulanger, J.-P., C. Menkes, and M. Lengaigne, 2004: Role of high- and low-frequency winds and wave reflection in the onset, growth and termination of the 1997–1998 El Niño. *Climate Dyn.,* **22,** 267–280.

Chang, P., B. Wang, T. Li, and L. Ji, 1994: Interactions between the seasonal cycle and the southern oscillation—Frequency entrainment and chaos in a coupled ocean-atmosphere model. *Geophys. Res. Lett.,* **21,** 2817–2820.

——, L. Ji, B. Wang, and T. Li, 1995: Interactions between the seasonal cycle and El Niño–Southern Oscillation in an intermediate coupled ocean–atmosphere model. *J. Atmos. Sci.,* **52,** 2353–2372.

Chelton, D. B., M. G. Schlax, M. H. Freilich, and R. F. Milliff, 2004: Satellite measurements reveal persistent small-scale features in ocean winds. *Science,* **303,** doi:10.1126/science.1091901.

Delworth, T. L., and Coauthors, 2006: GFDL's CM2 global coupled climate models. Part I: Formulation and simulation characteristics. *J. Climate,* **19,** 643–674.

Galanti, E., and E. Tziperman, 2000: ENSO's phase locking to the seasonal cycle in the fast-SST, fast-wave, and mixed-mode regimes. *J. Atmos. Sci.,* **57,** 2936–2950.

——, ——, M. Harrison, A. Rosati, R. Giering, and Z. Sirkes, 2002: The equatorial thermocline outcropping—A seasonal control on the tropical ocean–atmosphere instability strength. *J. Climate,* **15,** 2721–2739.

GFDL Global Atmospheric Model Development Team, 2004: The new GFDL global atmosphere and land model AM2–LM2: Evaluation with prescribed SST simulations. *J. Climate,* **17,** 4641–4673.

Giese, B. S., and D. E. Harrison, 1991: Eastern equatorial Pacific response to three composite westerly wind types. *J. Geophys. Res.,* **96** (Suppl.), 3239–3248.

Gnanadesikan, A., and Coauthors, 2006: GFDL's CM2 global coupled climate models. Part II: The baseline ocean simulation. *J. Climate,* **19,** 675–697.

Guilyardi, E., P. Delecleuse, S. Gualdi, and A. Navarra, 2003: Mechanisms for ENSO phase change in a coupled GCM. *J. Climate,* **16,** 1141–1158.

Harrison, D. E., 1987: Monthly mean island surface winds in the central tropical Pacific and El Niño. *Mon. Wea. Rev.,* **115,** 3133–3145.

——, and B. S. Giese, 1991: Episodes of surface westerly winds observed from islands in the western tropical Pacific. *J. Geophys. Res.,* **96,** 3221–3237.

——, and G. A. Vecchi, 1997: Westerly wind events in the tropical Pacific: 1986–1995. *J. Climate,* **10,** 3131–3156.

——, and N. K. Larkin, 1998: The ENSO surface temperature and wind signal: A near-global composite and time-series view, 1946–1995. *Rev. Geophys.,* **36,** 353–399.

——, and G. A. Vecchi, 1999: On the termination of El Niño. *Geophys. Res. Lett.,* **26,** 1593–1596.

——, and ——, 2001: El Niño and La Niña—Equatorial Pacific thermocline depth and sea surface temperature anomalies, 1986–98. *Geophys. Res. Lett.,* **28,** 1051–1054.

——, B. S. Giese, and E. S. Sarachik, 1990: Mechanisms of SST change in the equatorial waveguide during the 1982–83 ENSO. *J. Climate,* **3,** 173–188.

Jin, F.-F., J. D. Neelin, and M. Ghil, 1994: El Niño on the Devil's Staircase: Annual subharmonic steps to chaos. *Science,* **264,** 70–72.

Kiladis, G. N., and K. H. Straub, 2003: Ocean–atmosphere interaction within equatorially trapped atmospheric waves. Preprints, *12th Conf. on Interactions of the Sea and Atmosphere,* Long Beach, CA, Amer. Meteor. Soc., CD-ROM, J1.7.

Landsea, C. W., and J. A. Knaff, 2000: How much skill was there in forecasting the very strong 1997–98 El Niño? *Bull. Amer. Meteor. Soc.,* **81,** 2107–2119.

Larkin, N. K., and D. E. Harrison, 2002: ENSO warm (El Niño) and cold (La Niña) event life cycles: Ocean surface anomaly patterns, their symmetries, asymmetries, and implications. *J. Climate,* **15,** 1118–1140.

Lengaigne, M., J.-P. Boulanger, C. Menkes, P. Delecluse, and J. Slingo, 2004: Westerly wind events in the tropical Pacific and their influence on the coupled ocean-atmosphere system: A review. *Earth Climate: The Ocean-Atmosphere Interaction*, *Geophys. Monogr.,* Vol. 147, Amer. Geophys. Union, 49–69.

——, ——, ——, and H. Spencer, 2006: Influence of the seasonal cycle on the termination of El Niño events in a coupled general circulation model. *J. Climate,* **19,** 1850–1868.

Madden, R. A., and P. R. Julian, 1994: Observations of the 40-50 day tropical oscillation: A review. *Mon. Wea. Rev.,* **122,** 814–837.

McPhaden, M. J., 1999: Genesis and evolution of the 1997–98 El Niño. *Science,* **283,** 950–954.

Moorthi, S., and M. J. Suarez, 1992: Relaxed Arakawa–Schubert: A parameterization of moist convection for general circulation models. *Mon. Wea. Rev.,* **120,** 978–1002.

Penland, C., and P. D. Sardeshmukh, 1995: The optimal growth of tropical sea surface temperature anomalies. *J. Climate,* **8,** 1999–2024.

Philander, S. G. H., and A. D. Seigel, 1985: Simulation of the El Niño of 1982–1983. *Coupled Ocean Atmosphere Models,* J. Nihoul, Ed., Elsevier, 517–541.

Picaut, J., E. Hackert, A. J. Busalacchi, R. Murtugudde, and G. S. E. Lagerloef, 2002: Mechanisms of the 1997–1998 El Niño-La Niña, as inferred from space-based observations. *J. Geophys. Res.,* **107,** 3037, doi:10.1029/2001JC000850.

Reynolds, R. W., N. A. Rayner, T. M. Smith, D. C. Stokes, and W. Wang, 2002: An improved in situ and satellite SST analysis for climate. *J. Climate,* **15,** 1609–1625.

Song, Q., G. A. Vecchi, and A. Rosati, 2006: Indian Ocean variability in the GFDL Coupled Climate Model. *J. Climate,* in press.

Spencer, H., 2004: Role of the atmosphere in seasonal phase lock-

ing of El Niño. *Geophys. Res. Lett.,* **31,** L24104, doi:10.1029/2004GL021619.

Stouffer, R., and Coauthors, 2006: GFDL's CM2 global coupled climate models. Part IV: Idealized climate response. *J. Climate,* **19,** 723–740.

Takayabu, Y. N., T. Iguchi, M. Kachi, A. Shibata, and H. Kanzawa, 1999: Abrupt termination of the 1997–98 El Niño in response to a Madden-Julian Oscillation. *Nature,* **402,** 279–282.

Tziperman, E., L. Stone, M. A. Cane, and H. Jarosh, 1994: El Niño chaos: Overlapping of resonances between the seasonal cycle and the Pacific Ocean-Atmosphere oscillator. *Science,* **264,** 72–74.

——, M. A. Cane, and S. E. Zebiak, 1995: Irregularity and locking to the seasonal cycle in an ENSO prediction model as explained by the quasi-periodicity route to chaos. *J. Atmos. Sci.,* **52,** 293–306.

——, S. E. Zebiak, and M. A. Cane, 1997: Mechanisms of seasonal–ENSO interaction. *J. Atmos. Sci.,* **54,** 61–71.

——, M. A. Cane, S. E. Zebiak, Y. Xue, and B. Blumenthal, 1998: Locking of El Niño's peak time to the end of the calendar year in the delayed oscillator picture of ENSO. *J. Climate,* **11,** 2191–2199.

Vecchi, G. A., and D. E. Harrison, 2000: Tropical Pacific sea surface temperature anomalies, El Niño, and equatorial westerly wind events. *J. Climate,* **13,** 1814–1830.

——, and ——, 2003: On the termination of the 2002–03 El Niño event. *Geophys. Res. Lett.,* **30,** 1964, doi:10.1029/2003GL017564.

——, and ——, 2006: The termination of the 1997–98 El Niño event. Part I: Mechanisms of oceanic change. *J. Climate,* **19,** 2633–2646.

Wallace, J. M., T. P. Mitchell, and C. Deser, 1989: The influence of sea surface temperature on surface wind in the eastern equatorial Pacific: Seasonal and interannual variability. *J. Climate,* **2,** 1500–1506.

Wang, C., and J. Picaut, 2004: Understanding ENSO physics—A review. *Earth Climate: The Ocean-Atmosphere Interaction, Geophys. Monogr.,* Vol. 147, Amer. Geophys. Union, 21–48.

——, and R. H. Weisberg, 2000: The 1997–98 El Niño evolution relative to previous El Niño events. *J. Climate,* **13,** 488–501.

Wittenberg, A. T., A. Rosati, N.-C. Lau, and J. Ploshay, 2006: GFDL's CM2 global coupled climate models. Part III: Tropical Pacific climate and ENSO. *J. Climate,* **19,** 698–722.

Wyrtki, K., 1975: El Niño—The dynamic response of the equatorial Pacific Ocean to atmospheric forcing. *J. Phys. Oceanogr.,* **5,** 572–584.

Xie, S.-P., 1995: Interaction between annual and interannual variations in the equatorial Pacific. *J. Phys. Oceanogr.,* **25,** 1930–1941.

——, 2004: Satellite observations of cool ocean–atmosphere interaction. *Bull. Amer. Meteor. Soc.,* **85,** 195–208.

Zebiak, S. E., and M. A. Cane, 1987: A model El Niño–Southern Oscillation. *Mon. Wea. Rev.,* **115,** 2262–2278.

Zelle, H., G. Appeldoorn, G. Burgers, and G. J. van Oldenborgh, 2004: The relationship between sea surface temperature and thermocline depth in the eastern equatorial Pacific. *J. Phys. Oceanogr.,* **34,** 643–655.

Zhang, X., and M. J. McPhaden, 2006: Wind stress variations and interannual sea surface temperature anomalies in the eastern equatorial Pacific. *J. Climate,* **19,** 226–241.